doi:10.1016/j.jmb.2003.09.022 J. Mol. Biol. (2003) 333, 965–975

JMB

Available online at www.sciencedirect.com

SCIENCE DIRECT®

ELSEVIER

The Occupancy of Ions in the K^+ Selectivity Filter: Charge Balance and Coupling of Ion Binding to a Protein Conformational Change Underlie High Conduction Rates

Yufeng Zhou and Roderick MacKinnon*

Molecular Neurobiology and Biophysics, Howard Hughes Medical Institute and Rockefeller University, 1230 York Avenue, New York, NY 10021, USA

Potassium ions diffuse across the cell membrane in a single file through the narrow selectivity filter of potassium channels. The crystal structure of the KcsA K^+ channel revealed the chemical structure of the selectivity filter, which contains four binding sites for K^+. In this study, we used Tl^+ in place of K^+ to address the question of how many ions bind within the filter at a given time, i.e. what is the absolute ion occupancy? By refining the Tl^+ structure against data to 1.9 Å resolution with an anomalous signal, we determined the absolute occupancy of Tl^+. Then, by comparing the electron density of Tl^+ with that of K^+, Rb^+ and Cs^+, we estimated the absolute occupancy of these three ions. We further analyzed how the ion occupancy affects the conformation of the selectivity filter by analyzing the structure of KcsA at different concentrations of Tl^+. Our results indicate that the average occupancy for each site in the selectivity filter is about 0.63 for Tl^+ and 0.53 for K^+. For K^+, Rb^+ and Cs^+, the total number of ions contained within four sites in the selectivity filter is about two. At low concentrations of permeant ion, the number of ions drops to one in association with a conformational change in the selectivity filter. We conclude that electrostatic balance and coupling of ion binding to a protein conformational change underlie high conduction rates in the setting of high selectivity.

Keywords: potassium channel; KcsA; permeation; selectivity filter; ion occupancy

*Corresponding author

Introduction

All K^+ channels exhibit a set of characteristic ion conduction properties, of which, the presence of multiple potassium ions within the pore appears to be universal.[1–5] The 2.0 Å resolution structure of the KcsA K^+ channel, solved in the presence of 200 mM K^+, revealed multiple ion-binding sites in its permeation pathway:[6] two near the extracellular entryway where potassium ions reside just outside the filter, one halfway across the membrane in a water-filled cavity just internal to the filter, and four in the narrow 12 Å long selectivity filter where permeating ions bind in an essentially dehydrated state (Figure 1A). The selectivity filter, which is formed by the highly conserved K^+ channel signature sequence TVGYG, is the crucial structural element that facilitates the diffusion of potassium ions at rates approaching 10^8 ions per second under physiological electrochemical gradients.[5] In the selectivity filter, potassium ions are distributed nearly evenly over the four binding sites, which we refer to as positions 1–4, numbered from extracellular to intracellular (Figure 1B). Each ion-binding site is surrounded by eight oxygen atoms contributed by the backbone carbonyl groups of the TVGY sequence and the side-chain of the threonine residue.

The crystal structure of the KcsA K^+ channel shows clearly that the selectivity filter contains multiple discrete K^+-binding sites. However, the structure reveals only where potassium ions bind, it does not reveal how many ions bind at once.

Abbreviation used: SAD, single wavelength anomalous difference.

E-mail address of the corresponding author: mackinn@rockefeller.edu

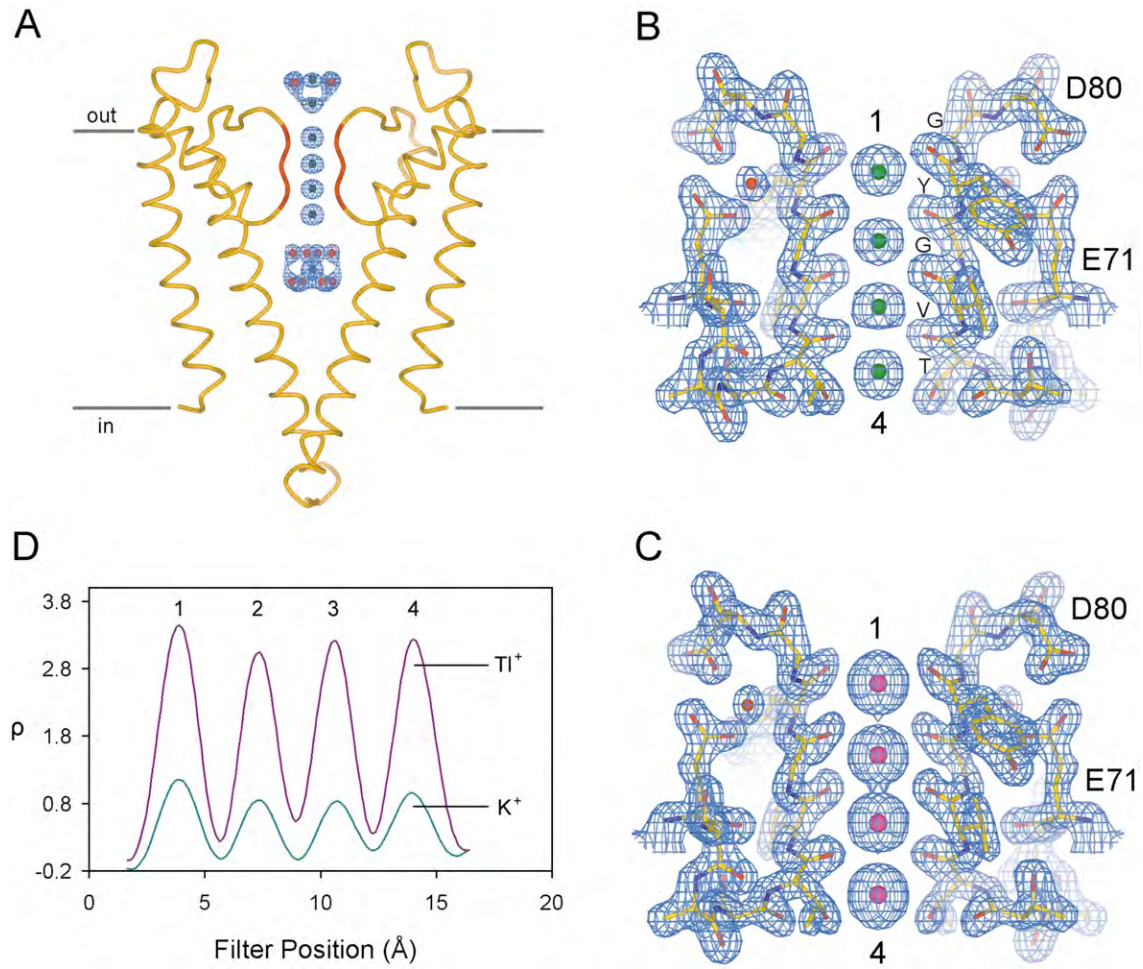

Figure 1. A, Ion-binding sites in the permeation pathway of KcsA. The gray lines indicate the external and internal membrane surfaces. Two diagonally opposed subunits of the tetrameric channel are shown as a yellow trace. The selectivity filter, corresponding to residue T75 through G79, is colored in red. K^+-binding sites along the permeation pathway are shown as green spheres, and water molecules surrounding the sites are shown as red spheres. The $F_o - F_c$ omit map (contoured at 3σ) validating the K^+ sites and the water molecules is shown as a blue mesh. B, The selectivity filter region (two subunits) of the structure shown in A. The selectivity filter signature sequence and the surrounding amino acid residues (from E71 to D80) are shown in ball-and-stick representation. The four K^+-binding sites in the filter are represented as green spheres and numbered 1 through 4, from extracellular to intracellular. The $2F_o - F_c$ electron density map validating the structure is colored in blue. C, Structure of the selectivity filter region in the presence of Tl^+. The structure, solved in 160 mM Tl^+, is represented in the same way as in B, except the Tl^+ binding sites are colored in pink. D, Positions of the Tl^+ and K^+-binding sites in the selectivity filter. The one-dimensional electron density (ρ) of Tl^+ and K^+ was obtained by sampling the difference Fourier omit maps along the central axis of the filter (as described in Methods). The level of the residue G79 α-carbon atom was set as zero on the *x*-axis. The four ion-binding sites are numbered in the same way as in B and C. Figures 1A–C, 3 and 5 were made with Bobscript[25,26] and Raster3D.[27]

The observed electron density is actually an average image of all accessible ion-binding states represented within the crystal. To understand the atomic details of the conduction mechanism we need to know how many ions reside in the filter; that is, what is the absolute occupancy. There are two reasons why it is difficult to determine the absolute occupancy of the ion-binding sites. First, binding sites not occupied by K^+ are likely to be occupied by water molecules,[7] and the electron density difference between a potassium ion (18 electrons) and a water molecule (ten electrons) is not great enough to distinguish easily their relative contributions to the diffraction pattern. Second, the Debye–Waller temperature factor (*B*-factor) and occupancy of an atom are correlated, making it difficult to quantify the occupancy. In a previous study, we inferred the ion occupancy by comparing the electron densities of K^+ and Rb^+ (Rb^+, like K^+, permeates potassium channels) within the selectivity filter at various concentrations of each ion.[8] Because the magnitude of electron density at the binding sites varies with ion concentration as well as the permeating ion species, comparison of K^+ and Rb^+ provided indirect information about ion occupancy. The results suggested that when the concentration of K^+ in solution is higher than about 20 mM there are two ions in the selectivity

filter at a given time, and that the two ions move in a concerted fashion between two configurations: a K^+–water–K^+–water configuration in which ions bind at positions 1 and 3, and a water–K^+–water–K^+ configuration in which ions bind at positions 2 and 4. When the K^+ concentration in solution is much less than 20 mM, ion occupancy in the filter decreases, and the filter switches to a different conformation.[6]

The comparative study of K^+ and Rb^+,[8] although very informative, did not enable the direct determination of absolute ion occupancy. Even with the heavier rubidium ion (36 electrons), the diffraction data did not permit us to separate the *B*-factor from the occupancy during refinement. Besides K^+ and Rb^+, three other ions are known to permeate potassium channels: Tl^+, NH_4^+ and Cs^+.[9–11] To obtain the absolute occupancy of ions, the best option is to crystallize KcsA in Tl^+ instead of K^+, and measure the occupancy of the thallium ions. Tl^+ is an excellent substitute for K^+ because it permeates potassium channels, and because its radius (1.4 Å) is more similar to that of K^+ (1.33 Å) than is the radius of other known permeating ions. For crystallographic purposes, Tl^+ offers distinct advantages: its 80 electrons provide a strong diffraction signal and at certain X-ray wavelengths it produces an anomalous signal, which provides additional information about Tl^+ in the crystal. These features of Tl^+ allow us to determine the absolute occupancy of ions in the selectivity filter more accurately.

The primary goal of this study is to determine how many ions bind in the selectivity filter at once. We achieved this goal in four steps. First, we solved the structure of KcsA in Tl^+ and compared it with the structure in K^+ to confirm that the two complexes have similar structures. Second, we applied two different approaches to determine the absolute Tl^+ occupancy. Third, we used the Tl^+ occupancy as a standard to estimate the occupancy of potassium ions as well as Rb^+ and Cs^+. Fourth, we determined the Tl^+ occupancy at different concentrations of Tl^+ and observed how the filter structure changes as a function of the number of ions present in the filter. Our findings lead us to two important conclusions: first, that two potassium ions reside in the conductive conformation of the selectivity filter, probably as a result of electrostatic balance between potassium ions and the protein, and second, that the two-ion (conductive) state is achieved through a protein conformational change of the filter upon binding of the second potassium ion. These conclusions form the basis of understanding high conduction rates in the setting of high selectivity in K^+ channels.

Results

Structure of KcsA in Tl^+

In order to obtain high-resolution structures, KcsA was co-crystallized with an antibody Fab fragment. The Fab fragment provides in the crystal well-ordered protein–protein contacts necessary for high-quality X-ray diffraction. The Fab binds to the turret of the channel at the extracellular side, but leaves the channel structure and its ion permeation pathway unperturbed.[6] Although the KcsA structures in this study are structures of KcsA–Fab complexes, we focus only on the channel region, and for simplicity refer to these as structures of KcsA.

We determined a structure in 160 mM Tl^+ at 1.9 Å resolution (80 mM Na^+ was present in the crystallization condition to maintain ionic strength). The model was refined to free and crystallographic residuals of 22.8% and 20.8%, respectively, and contains 534 amino acid residues, 360 water molecules, two partial lipid molecules and five thallium ions (four in the selectivity filter and one in the cavity; the Tl^+ at the extracellular entryway to the filter was excluded because its occupancy is low). This structure is nearly identical with the structure of KcsA in 200 mM K^+ (Figure 1A), with a root mean square deviation (rmsd) of 0.43 Å for the entire channel and 0.12 Å for the selectivity filter region, from residue E71 to D80 (Figure 1B and C). We compared the ion distribution of Tl^+ and K^+ in the selectivity filter. As shown in the one-dimensional maps of electron density sampled along the axis of the filter (Figure 1D), Tl^+ and K^+ bind at essentially identical positions, and both are distributed nearly evenly over four positions, sites 1–4. The filter conformation and distribution of K^+ (Figure 1B) and Tl^+ (Figure 1C) corresponds to the high-K^+ structure, described in an earlier study.[6] Therefore, we refer to the structure shown in Figure 1C as the high-Tl^+ structure in the following discussion.

Tl^+ occupancy

The near identity of the structures in Tl^+ and K^+ and the same ion distribution profiles indicate that Tl^+ is a good K^+ analog for estimating ion occupancy in the selectivity filter. We applied two different approaches to quantify the Tl^+ occupancy, both employing the same data set that provided the high-Tl^+ structure discussed above (Figure 1C). The data were strong to 1.9 Å resolution, complete (Table 1), and contained an anomalous signal from the thallium ions. The anomalous signal, explained in more detail below, plays a role in both of our approaches for estimating ion occupancy. Also, in both approaches, the effect of *B*-factors, which in theory account for the thermal motion of atoms, must be considered very carefully, because *B*-factors and atom occupancies are always correlated.

In our first approach we calculated a set of structure factors (F_c) based on the high-Tl^+ structure, and compared these with the experimental data (F_o). The refinement procedure adjusts the ion occupancies in the structure to minimize the

Table 1. Crystallographic data statistics

Salt concentration					
$TlNO_3$ (mM)	$NaNO_3$ (mM)	Resolution (Å)	R_{sym}[a]	Completeness (%)	Refinement statistics R_{free}/R_{work} (%)[b]
3	237	2.9	0.095	92.9	24.3/21.2
25	215	2.8	0.136	99.8	27.3/23.8
65	175	2.3	0.083	100	29.2/27.1
80	160	2.9	0.103	96.6	30.6/26.1
100	140	2.4	0.093	99.8	24.9/21.8
160	80	1.9	0.069	97.1	22.8/20.8
240	0	2.8	0.107	96.3	28.1/23.1
RbCl (mM)					
200		2.4	0.074	99.1	23.8/21.8
CsCl (mM)					
200		2.4	0.071	98.8	24.9/21.9

[a] $R_{sym} = \sum|I_i - \langle I_i\rangle|/\sum I_i$, where $\langle I_i\rangle$ is the average intensity of symmetry-equivalent reflections.
[b] $R = \sum|F_o - F_c|/\sum F_o$, 5% or 10% of the data that were excluded in refinement were used in the R_{free} calculation.

residual between F_c and F_o. Since atoms interacting with each other are expected to have similar *B*-factors, we made the assumption that the *B*-factors of the thallium ions (B_{Tl^+}) in the selectivity filter should be very close to the *B*-factors of the immediately surrounding atoms (which includes all backbone atoms of the selectivity filter TVGY sequence and the side-chain atoms of the Thr residue). In the first half-cycle of refinement we obtained *B*-factors for each of the surrounding atoms by initially setting the occupancy of all Tl^+ sites in the model either to 1.0 or 0.5, before carrying out individual *B*-factor refinement on all atoms in the model. Next we calculated the average *B*-factor value of the atoms surrounding the Tl^+ sites. In the second half-cycle, the B_{Tl^+} were set at this averaged value; then individual occupancy refinement was carried out for each Tl^+ site. Several cycles of alternating *B*-factor and occupancy refinement were carried out using both experimental amplitudes and anomalous differences (see Methods). One additional adjustment should be considered: if a site is not occupied by an ion, it is likely to be occupied by a water molecule. Since this refinement approach does not distinguish the relative contribution of an ion and a water molecule to the X-ray diffraction, the occupancy obtained should be the apparent ion occupancy ($\theta_{ion,app}$). It is related to the true ion occupancy (θ_{ion}) according to the equation:

$$\theta_{ion,app} = [\theta_{ion}N_{ion} + (1 - \theta_{ion})N_{water}]/N_{ion} \quad (1)$$

where N_{ion} and N_{water} are the number of electrons in the ion ($N_{Tl^+} = 80$) and water ($N_{water} = 10$), respectively. The results of the refinement showed that after three cycles, the average apparent occupancy of Tl^+ ($\theta_{Tl^+,app}$) for the four ion-binding sites in the filter converged to about 0.8 per site (Figure 2A), corresponding to 0.75 for θ_{Tl^+} and 0.25 for water ($1 - \theta_{Tl^+}$), yielding an average of three thallium ions and one water molecule in the filter at a given time. The average *B*-factors of the thallium ions and of the atoms surrounding the Tl^+ sites remained about 24 $Å^2$ through each cycle of refinement.

The above refinement method carries an unknown systematic error that depends on the

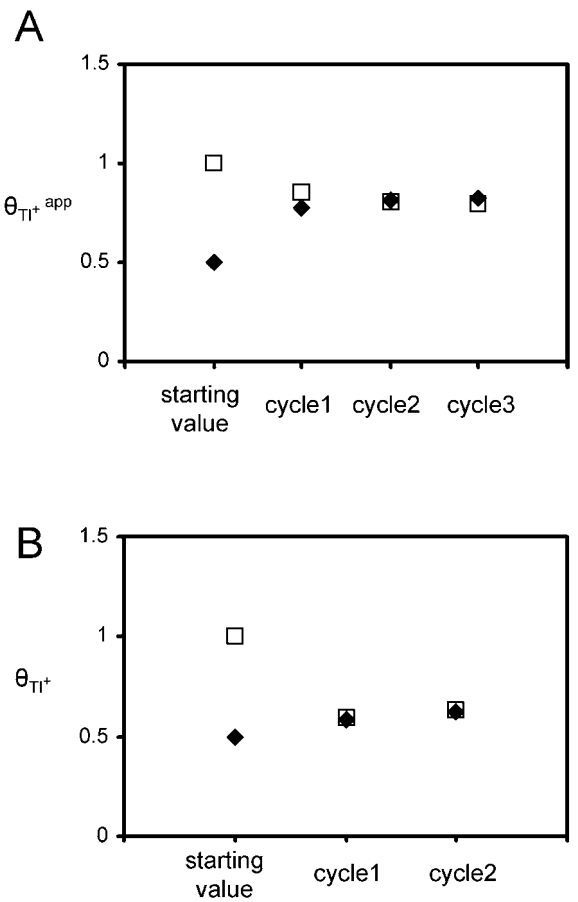

Figure 2. Refinement of Tl^+ occupancy in the selectivity filter using the first approach (A) and the second approach (B) as described in Results. The data represent the average occupancy of the four Tl^+ sites in the filter obtained from each cycle of the refinement. For each approach, the refinement was carried out twice with the initial occupancy value set at either 1 (open square) or 0.5 (filled diamond).

accuracy of the structure model. Since the refinement compares an experimental structure factor set against a theoretical structure factor set derived from a model, the error of every atom in the model (over 4000) will contribute to the error in occupancies calculated for the binding sites. Therefore, the conclusion requires verification by an alternative procedure. For this purpose, we carried out single wavelength anomalous difference (SAD) refinement.[12,13] Anomalous scattering occurs when the photon energy of an X-ray beam causes changes in the quantum state of the electrons within an atom, such as Tl^+ at a wavelength of 0.95 Å. As a consequence, the measured structure factors will have a special property: pairs of structure factors (called Friedel pairs $F_{h,k,l}$ and $F_{-h,-k,-l}$) whose amplitude are normally equal become unequal. The difference in amplitude, called the anomalous difference, arises only from the thallium ions and not the water or protein atoms. The fundamental advantage to this second approach is that the anomalous difference depends only on 25 parameters to be refined; the location (x, y, z), *B*-factor and occupancy of the five Tl^+ positions; four in the filter and one in the cavity.

The refined model of the protein structure made one important contribution to the SAD refinement by providing a scale factor to place the entire data set on an absolute scale through comparison of F_c and F_o (see Methods). Use of the model for this purpose is not very sensitive to small errors in the model and, as one should expect, the scale factor derived using the model was within 10% of that obtained through Wilson statistical analysis using the TRUNCATE function in CCP4.[14] On the basis of our first refinement procedure (above), we set the initial *B*-factors at 24 $Å^2$ and the initial occupancies to be either 1.0 or 0.5. Cycles of SAD refinement were carried out using a protocol similar to that described in our first approach to occupancy refinement. Using all data within the resolution range 20–2.0 Å, the average occupancy for the four Tl^+ sites in the selectivity filter was 0.63 after two cycles of refinement (Figure 2(B)), corresponding to an average of 2.5 thallium ions in the filter at any given time. Since water molecules do not generate an anomalous signal, this result required no further correction. This refinement approach includes an unknown error, because the anomalous difference between two structure factors is small, typically only a small percentage of the structure factors. The accuracy of the refinement depends on the accuracy of the data measurement.

Two different methods for estimating Tl^+ occupancy in the selectivity filter of KcsA yielded an average Tl^+ occupancy of 0.75 for each site (three ions total in the filter) or 0.63 for each site (2.5 ions total in the filter): the two results are not very different. Since the second method depends on fewer parameters, we think it is more accurate. In the following analysis we assume an occupancy of 0.63 for Tl^+ at each position in the filter.

Occupancy of K^+, Rb^+ and Cs^+ in the selectivity filter

The above refinement procedures require high-resolution data, electron-dense ions, and strong anomalous scattering. Our data for KcsA crystallized in permeant ions other than Tl^+ could not meet this standard. Therefore, we used the Tl^+ occupancy as a reference to estimate the occupancy of K^+ as well as Rb^+ and Cs^+. That is, we compare the electron density peaks of K^+, Rb^+ and Cs^+ to that of Tl^+, and use the known Tl^+ occupancy to estimate the occupancy of the other ions.

We used the structure of KcsA in 200 mM K^+ determined previously (Figure 1B),[6] and the structure in 160 mM Tl^+ as described above (Figure 1C). We determined the structures of

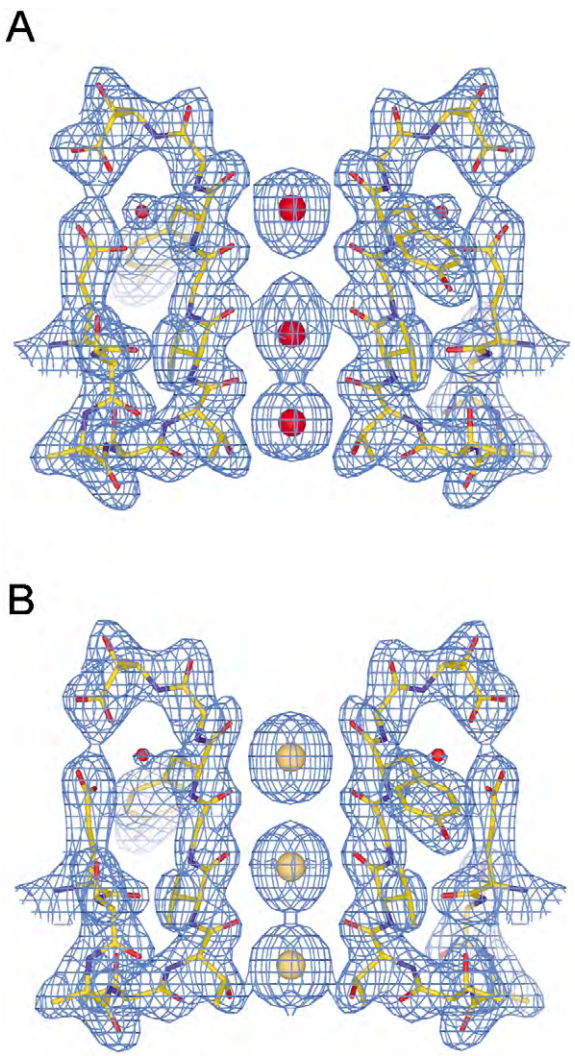

Figure 3. Structure of the selectivity filter region in the presence of Rb^+ (A) or Cs^+ (B). Both structures were solved in the presence of the corresponding ion at a concentration of 200 mM. The selectivity filter region of the structures are shown in the same way as in Figure 1B and C, except the Rb^+ binding sites are represented as red spheres and the Cs^+-binding sites are represented as gold spheres.

KcsA in 200 mM Rb^+ and 200 mM Cs^+ at 2.4 Å resolution (Table 1). The protein structures in Rb^+ and Cs^+ are very similar to the high-K^+ or the high-Tl^+ structures (the rmsd between the structure in Rb^+ and in high-K^+ is 0.30 Å for the entire channel and 0.23 Å for the selectivity filter region, and the rmsd between the structure in Cs^+ and in high-K^+ is 0.33 Å for the entire channel and 0.37 Å for the selectivity filter region), except there are only three major occupied ion positions in the selectivity filter instead of four (Figure 3).

We placed each data set on a common scale and calculated one-dimensional electron density maps sampled along the axis of the filter (Figure 4A). The maps were calculated using coefficients $(F_o - F_c)$, where F_c is the inverse-Fourier transform of a refined model in which the selectivity filter ions and protein atoms have been omitted, and phases from a model refined in the absence of selectivity filter ions (with the filter harmonically restrained). The area of each peak in Figure 4A, which under certain assumptions (see Methods) is proportional to the apparent ion occupancy ($\theta_{ion,app}$), was integrated and converted to ion occupancy assuming that each Tl^+ peak represents 0.63 Tl^+, and that a water molecule is present at a site when an ion is not (equation (1)). The results (Figure 4B) suggest that the K^+ occupancy in the selectivity filter is about 0.53 per site (average over four sites), in agreement with our previous conclusion that there are two potassium ions in the filter at a given time.[8] The total ion occupancy for Rb^+ and Cs^+ is also about two, even though these larger ions distribute differently in the filter than K^+ and Tl^+. This finding implies that the total positive charge in the selectivity filter is conserved near two. Considering that the selectivity filter contains many oxygen atoms, all pointing a partial negative charge towards the narrow ion pathway, we suggest that two permeating ions serve as "counter-charges", which are required to maintain the structural stability of the filter.

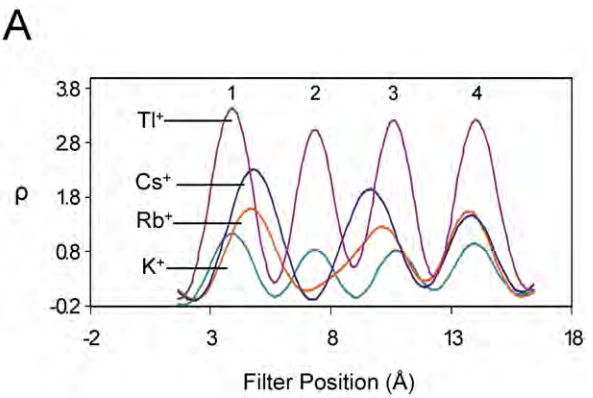

B

	K^+	Rb^+	Cs^+	Tl^+
position1	0.58	0.81	0.83	0.69
position2	0.51			0.56
position3	0.48	0.73	0.69	0.60
position4	0.54	0.67	0.40	0.67
total number of ions in the filter	2.1	2.2	1.9	2.5

Figure 4. K^+, Rb^+ and Cs^+ occupancy in the selectivity filter. A, The relative electron density (ρ) of K^+, Rb^+, Cs^+ and Tl^+. The one-dimensional electron density of Rb^+ and Cs^+ was obtained and plotted in the same way as in Figure 1D. The electron density of K^+ and Tl^+ are shown for comparison. B, Occupancy of Rb^+, Cs^+ and Tl^+ at each position was deduced from the areas of the peaks in A, using average Tl^+ occupancy of 0.63 at each site as the absolute scale. The occupancy of K^+ at each position was deduced using the same method except the one-dimensional electron density was calculated using higher-resolution data (up to 2.0 Å instead of 2.4 Å resolution).

Structure of the selectivity filter at low concentrations of ion

Without the counter-charges provided by permeating ions, the selectivity filter changes its conformation. At 3 mM K^+ (and additional 200 mM Na^+ to maintain ionic strength) it was shown in a previous study that the backbone carbonyl group of Val76 rotates away from the center of the pore, that the C^α of Gly77 faces towards the pore, and that ions are absent at positions 2 and 3 (Figure 5A). We refer to this structure as the low-K^+ structure. The difference between the high-K^+ and low-K^+ structure is significant at the selectivity filter region, whereas the remainder of the channel is essentially unchanged.[6]

In 25 mM Tl^+ (and additional 215 mM Na^+ to maintain ionic strength) the filter adopts the low-Tl^+ structure, which is nearly identical with that observed in 3 mM K^+ (Figure 5B): comparing the low-Tl^+ and low-K^+ structure, we find that the rmsd is 0.49 Å for the entire channel and 0.46 Å for the selectivity filter region. Since Tl^+ is more electron-dense than K^+, we used structures with Tl^+ to study the relationship between ion occupancy and filter conformation. We analyzed seven structures in concentrations of Tl^+ ranging from 3 mM to 240 mM; in each case, the ionic strength was kept constant by the addition of Na^+ (Table 1). One-dimensional electron density maps for five of the structures are shown in Figure 6A. The high-Tl^+ structure, similar to the high-K^+ structure, was observed at concentrations higher than 100 mM Tl^+, and the low-Tl^+ structure was observed at concentrations lower than 65 mM Tl^+. At 80 mM Tl^+ the electron density of the channel is poorly defined for the selectivity filter atoms but well defined for the remainder of the channel (not shown). The apparently disordered selectivity filter at 80 mM Tl^+ probably represents an average of low and high concentration structures within

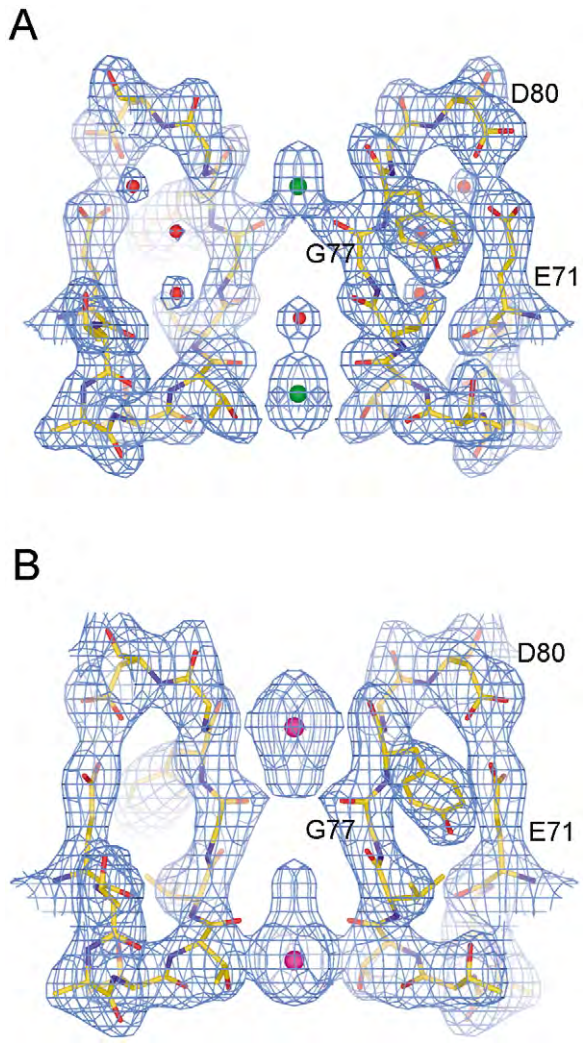

Figure 5. The selectivity filter conformation in A 3 mM K^+ or B 25 mM Tl^+. Both structures are presented the same way as in Figure 1B and C.

the crystal; that is, a point of transition from one structure to the other.

We could not refine accurately the ion occupancy in the low-Tl^+ structures because the resolution of the data was not sufficiently high and because the anomalous differences were too small. Therefore, we estimated the occupancy using the same approach used for K^+, Rb^+ and Cs^+. Data sets were placed on a common scale, maps calculated, and peak areas were integrated and the corresponding occupancy of each site was computed (Figure 6B). The total number of ions in the selectivity filter was obtained by summing the occupancies of all four positions in the filter. As shown in Figure 6C, the total number of ions in the filter is always greater than two for the high-Tl^+ conformation and less than one for the low-Tl^+ conformation. A sharp transition from one to two ions accompanies the transition from the low to the high Tl^+ conformation of the filter. Given the near identity of the KcsA structures in K^+ and Tl^+ in both the low- and high-ion conformations, we

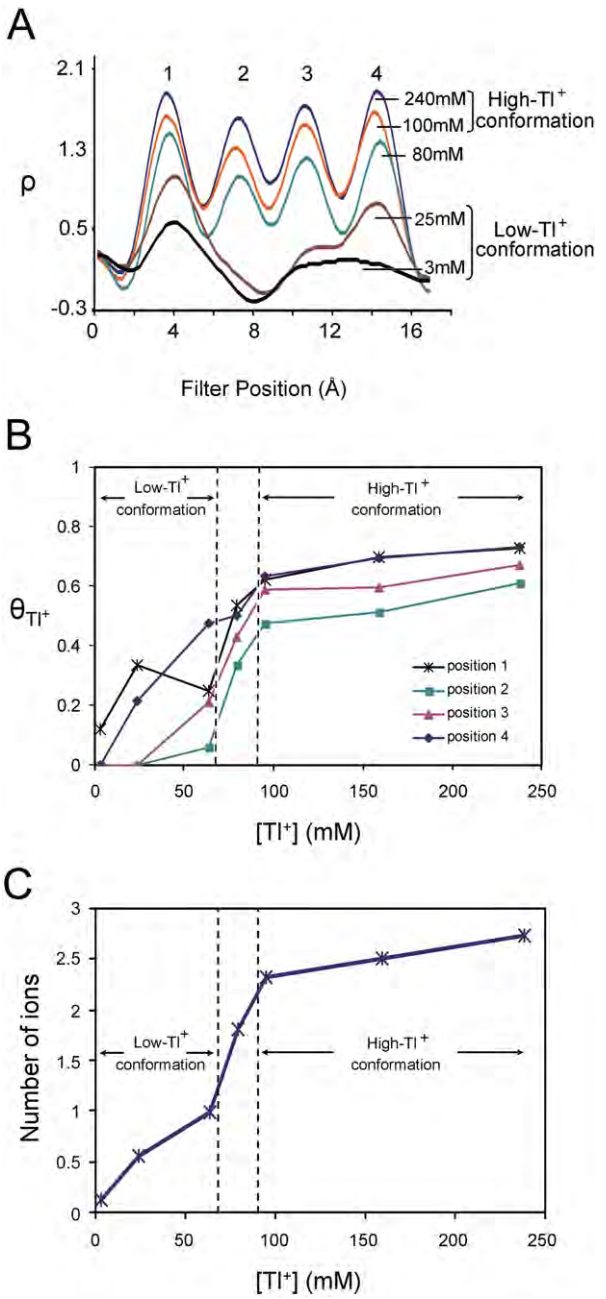

Figure 6. Correlation between the ion occupancy in the filter and the conformation of the filter. Seven structures of KcsA were solved in various concentrations of Tl^+. The selectivity filters in three of them adopted the high-Tl^+ conformation shown in Figure 1C and another three adopted the low-Tl^+ conformation shown in Figure 5B. In one structure, solved in 80 mM Tl^+, the electron density of the filter was disordered. In each of the following panels, the filter conformation of the corresponding structure was indicated. A, One-dimensional electron density (ρ) profiles of five structures obtained and plotted in the same way as Figure 1D. B, Change of Tl^+ occupancy at every position with respect to the solution concentration of Tl^+. The occupancies were deduced using the same approach as that used in Figure 4. C, Change of total number of ions in the filter with respect to concentration of Tl^+. The total number of ions in the selectivity filter (*y*-axis) was obtained by summation of the occupancies at all four positions (as shown in B).

conclude that the correlation between ion occupancy and filter conformation is the same when the channel is in K^+.

Discussion

Ion occupancy in the K^+ selectivity filter

In this study we measured the absolute occupancy of ions in the selectivity filter of a K^+ channel. Occupancy was studied by X-ray crystallography using Tl^+, an electron-dense K^+ analog that produces an anomalous diffraction signal. We conclude that an average of 2.5 thallium ions are present in the selectivity filter at a given time, and that the ions are distributed fairly evenly over four equally spaced ion-binding sites. Using Tl^+ as an electron density standard, we estimate that an average of about 2.0 ions, K^+, Rb^+ or Cs^+, reside in the filter at once. Like Tl^+, K^+ is distributed evenly over the four sites. On the basis of previous work, the even distribution, or nearly equal occupancy at all four sites, has been attributed to a nearly balanced mixture of two configurations: K^+–water–K^+–water (1–3 configuration) and water–K^+–water–K^+ (2–4 configuration) in sites 1 to 4 within the crystal.[8] The estimate for K^+ occupancy of about 0.5 at each site made in this study is in good agreement with the proposed conduction mechanism.

The Tl^+ occupancy from high-resolution diffraction data containing an anomalous signal is direct, whereas the K^+ occupancy determination is more indirect, based on electron density integration and Tl^+ as a standard. It is interesting, however, that this indirect approach yielded essentially the same total occupancy, around 2.0, for K^+, Rb^+, and Cs^+. The consistency in total occupancy for the alkali metal cations argues that the indirect approach is probably fairly accurate. We do not know whether the slightly higher occupancy estimated for Tl^+ (2.5 ions *versus* 2.0 for the alkali metals) is significant. It is possible that the higher electronic polarizability of Tl^+ compared to the alkali metals could account for a slightly stronger binding energy and higher overall occupancy.[15] If this is the case, then Tl^+ would sometime occupy adjacent positions within the selectivity filter. However, the difference between 2.5 for Tl^+ and 2.0 for the alkali metal cations is small and may not be significant. The most important conclusion from the occupancy measurements is that they demonstrate unequivocally that multiple potassium ions, on average about two, reside simultaneously in the short selectivity filter of K^+ channels.

Effect of ionic radius on binding in the filter

K^+, Tl^+, Rb^+ and Cs^+ form a series of permeant cations with radius 1.33 Å, 1.40 Å, 1.48 Å, and 1.69 Å, respectively. In contrast to K^+ and Tl^+, Rb^+ and Cs^+ reside predominantly at only three positions in the filter; their larger ionic radius clearly affects their distribution even though the protein structure of the filter is very similar for all four ions (Figures 1 and 3). In trying to understand the anomalous distribution of the larger ions (compared to K^+ or Tl^+) we have to consider that ions and water molecules are not expected to bind independently to sites within the filter. It is more realistic to think of the filter as a "binding site" for a queue of ions and water (i.e. the "substrate" is a queue of two ions and two water molecules, most often in an alternating arrangement). With such a picture in mind, we speculate that the length of the queue may be too long when the ions are Rb^+ or Cs^+, or possibly that the "structural periodicity" of the ion–water queue is suboptimal in the case of Rb^+ or Cs^+. The filter with its four very similar, equally paced sites is a highly periodic structure; it might be significant that K^+ and Tl^+ both have a radius that is very close to that of an oxygen atom, that is, around the size of a water molecule, allowing a queue with regular spacing that is possibly in register with sites in the selectivity filter.

Charge balance in the filter

The smaller (K^+) and larger (Cs^+) permeant ions have very different distributions in the filter but the total number of ions residing in the filter at a given time is the same for both, about 2.0. We think that this finding reflects the importance of charge balance within the filter, which directs 20 oxygen atoms toward the center of a 12 Å long, narrow cylinder, and each oxygen atom is associated with a partial negative charge. Thus, the ions seem to serve as counter-charges necessary for maintaining the filter's three-dimensional structure. Charge balance is also an important feature of the proposed conduction mechanism: two potassium ions (separated by one water molecule) oscillate between 1–3 and 2–4 configurations until a third potassium ion enters from one side and the ion–water queue shifts, displacing a potassium ion from the opposite side.[8] In other words, two potassium ions are stable in the filter, but three ions, representing a transition state, would be less stable.

Effect of ion occupancy on the structure of the selectivity filter

A systematic study of the selectivity filter structure determined at seven different concentrations of Tl^+ shows that it adopts two distinct and well-defined structures at low (65 mM and below) and high (100 mM and above) concentrations (Table 1; Figures 5 and 6). This does not mean to say that the selectivity filter is "floppy", but rather that it exists in one of two conformations that are associated with one (or fewer) and two ions, and that the equilibrium between the two structures is driven by the association of the second ion to the singly occupied filter (Figure 6C). The low and

high-Tl^+ structures are essentially identical with the low and high-K^+ structures described previously,[6] but the transition between the two conformations has a midpoint closer to 20 mM in K^+ and to 80 mM in Tl^+.[8] The low-ion structure is most certainly not occurring during the ion conduction "cycle", after all, physiological concentrations of K^+ surrounding an open, conducting K^+ channel are well above the concentration range at which the structural transition takes place, and such a large conformational change is probably incompatible with conduction rates approaching 10^8 K^+ per second. But, for reasons outlined below, we do think that the observed conformational change is directly related to the K^+ channel's ability to conduct K^+ at very high rates.

Ion-binding-induced conformational change as a principle for high conduction rates

The most remarkable feature of the K^+ channel is its high conduction rate in the setting of extraordinary selectivity for K^+ over Na^+. High selectivity would seem to imply near-optimal coordination sites for K^+ that should give rise to high-affinity binding. How then do potassium ions move through the pore at rates approaching the diffusion limit? One explanation for the existence of high conduction rates in the setting of high selectivity is electrostatic repulsion between ions. This mechanism was first proposed by electrophysiologists,[1,16–18] and is supported strongly by the demonstration of two potassium ions inside the selectivity filter of K^+ channels.

We think that the ion-dependent conformational change within the selectivity filter implies a second mechanism for maintaining high conduction rates in a selective ion channel. What are the energetic consequences of an ion-induced conformational change? To answer this question, imagine that the selectivity filter did not undergo a conformational change, but instead maintained its high K^+ (conductive) conformation even at low concentrations of K^+ when it became singly occupied. Figure 7 illustrates this idea. We observe experimentally a protein conformational change when the occupancy goes from 1.0 to 2.0 ions (Figure 7A), but hypothetically we might have observed an occupancy increase within a pre-formed high-ion structure; that is, without an associated conformational change (Figure 7B). It is evident that the observed protein conformational change has a simple thermodynamic consequence: the affinity of ions in the doubly occupied (conductive) state will be lowered. In other words, the "energy cost" of the conformational change to achieve the conductive state is "paid for" by some of the free energy of ion binding, resulting in weaker binding. The very same concept has been considered at length for substrate catalysis by enzymes to explain high substrate specificity in the setting of a high K_m.[19] We think that this same principle applies to the K^+ channel. It rationalizes our observation of two ion-dependent conformations of the selectivity filter, and explains how K^+ can bind selectively but not too tightly.

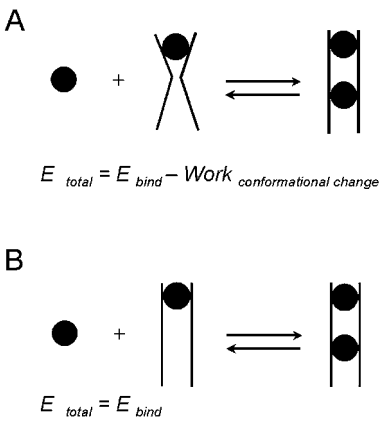

Figure 7. Transition between low- and high-ion structures may be important for high conduction rates. A, Experimentally observed conformational change when the occupancy in the selectivity filter changes from 1.0 to 2.0 ions. B, In a hypothetical case, the selectivity filter is held in a pre-formed, high-ion structure. Two ions will bind with lower affinity if binding energy is used to perform work to change the protein's conformation.

Methods

Protein purification

To prepare the KcsA–Fab complex in Tl^+, the complex was purified in 50 mM Hepes (pH 7.5), 150 mM KNO_3 and 5 mM detergent (decylmaltoside; DM) as described.[6,20] Before setting up crystallization trials, the complex was dialyzed against a buffer containing 50 mM Hepes (pH 7.5), 5 mM DM and the desired amount of $TlNO_3$. The ionic strength of all the dialysis buffers were kept constant by addition of $NaNO_3$.

To prepare the KcsA–Fab complex in Rb^+ and Cs^+, the complex was purified in 50 mM Tris (pH 7.5), 150 mM KCl and 5 mM DM. Before setting up crystallization trials, the complex was dialyzed against a buffer containing 50 mM Tris (pH 7.5), 5 mM DM and either 150 mM RbCl or 150 mM CsCl.

Crystal preparation

Crystals of space group *I*4 were grown at 20 °C by equilibrating a 1:1 mix of the protein and reservoir solution against the reservoir (18–25% (w/v) PEG400, 50 mM magnesium acetate, 50 mM sodium acetate at pH 5.4 or Hepes at pH 7.0) using the sitting-drop method. Cryo-protection of the crystal was achieved through vapor-diffusion by increasing the concentration of PEG 400 in the reservoir slowly to 40%. The salt concentration in the drop increased during this process; for crystals grown in Tl^+, the final free Tl^+ concentration was estimated to be 3 mM, 25 mM, 65 mM, 80 mM, 100 mM, 160 mM, or 240 mM; for crystals grown in Rb^+ or Cs^+, the final ion concentration was estimated to be 200 mM.

Crystallographic analysis

Data were collected at station A1 and F1 of the Cornell High Energy Synchrotron Source, and at station X-25 of the National Synchrotron Light Source (Brookhaven National Laboratory) (Table 1). The data were processed with Denzo, Scalepack[21] and the CCP4 package.[14] All the structures were solved by molecular replacement using the published KcsA–Fab structure (PDB code 1K4C). The models were refined by several cycles of manual rebuilding (using program O[22]), simulated annealing, minimization and individual *B*-factor refinement using CNS.[23]

One-dimensional electron density profiles were obtained as described.[8] Briefly, for comparing the ion distribution in different permeating ions (K^+, Tl^+, Rb^+ and Cs^+), all the data sets were scaled to 2.4 Å resolution using the K^+ data as the reference set; for comparing the ion distribution in different concentrations of Tl^+, all the data sets were scaled to 3.0 Å using the 160 mM Tl^+ data set as the reference set. All models, without ions, were refined against their corresponding data set, and the selectivity filter residues (TVGYG) were removed from the model before difference Fourier maps were calculated. One-dimension electron density profiles were obtained by sampling the difference maps along the central axis of the selectivity filter using MAPMAN.[24] Removing the selectivity filter before map calculation causes only a small change in the model phases, but can reduce the local error in the selectivity filter region of the electron density map significantly.

Occupancy was estimated for K^+, Rb^+ and Cs^+ by comparing one-dimensional electron density maps with Tl^+ as a standard of known occupancy (see below). To test the validity of using one-dimensional maps for this purpose, we calculated structure factors and electron density maps from atomic models containing the different ions. We found that the relative peak areas in one-dimensional electron density maps calculated from these model maps were nearly proportional to the relative number of electrons in the model ion. One-dimensional maps take advantage of the straight line of ions in the K^+ channel, and allow us to avoid electron density overlap with protein oxygen atoms that line the perimeter of the selectivity filter.

Tl^+ occupancy refinement

Ion occupancy refinement was carried out using data collected on the crystal grown in 160 mM $TlNO_3$. Before occupancy refinement, the model structure was refined to an R_{free} and R_{work} of 22.8% and 20.8%, respectively. All measured data between the resolution limits of 20 and 1.9 Å were used for the refinement (except for a random set of reflections (10%) used for calculation of R_{free}), and the Friedel's pairs of the data were averaged. Then the Friedel's pairs were separated, and all measured data between the resolution limits of 20 and 2.0 Å were used to refine the Tl^+ occupancy (except 10% for R_{free} calculation). Two refinement approaches were used (see Results for details). For both approaches, the wavelength-dependent parameters of the Tl^+ scattering factors f_{Tl} (a function of f' and f'') were calculated using CROSSEC from the CCP4 suite.[14] An f' of -9.731 electrons and f'' of 9.636 electrons were used for the occupancy refinement. In order to obtain absolute occupancy using the SAD refinement approach, the experimental data must be placed on the absolute scale. To do so, we first applied a scale factor obtained from the Wilson analysis of our data (using the TRUNCATE function in CCP4.[14] Next we calculated a set of structure factors (F_c) using the refined structure model described above, and scaled our experimental data (F_o) to the calculated data. The structure factor calculation, scaling of data sets, and occupancy refinement were carried out using CNS,[23] unless specified otherwise.

Protein Data Bank accession codes

The atomic coordinates and structure factors for the high Tl^+, low Tl^+, Rb^+, and Cs^+ complexes are deposited with the Protein Data Bank under PDB codes 1R3J, 1R3K, 1R3I, and 1R3L, respectively.

Acknowledgements

We thank the staff at CHESS A1 and F1 and BNL X-25 for assistance in data collection, A. Kaufman for help in protein purification, members of the MacKinnon laboratory for helpful discussions, F. Valiyaveetil, M. Zhou and S. Lockless for advice on the manuscript, and F. Weis-Garcia for assistance with monoclonal antibodies. This work was supported by NIH grant GM47400. R.M. is an Investigator in the Howard Hughes Medical Institute.

References

1. Neyton, J. & Miller, C. (1988). Discrete Ba^{2+} block as a probe of ion occupancy and pore structure in the high-conductance Ca^{2+}-activated K^+ channel. *J. Gen. Physiol.* **92**, 569–586.
2. Vestergaard-Bogind, B., Stampe, P. & Christophersen, P. (1985). Single-file diffusion through the Ca^{2+}-activated K^+ channel of human red-cells. *J. Membr. Biol.* **88**, 67–75.
3. Begenisich, T. & Deweer, P. (1980). Potassium flux ratio in voltage-clamped squid gient-axons. *J. Gen. Physiol.* **76**, 83–98.
4. Hodgkin, A. L. & Keynes, R. D. (1955). The potassium permeability of a giant nerve fibre. *J. Physiol. (London)*, **128**, 61–88.
5. Hille, B. (1992). *Ionic Channels of Excitable Membranes*, Sinauer Associates, Sunderland, MA.
6. Zhou, Y. F., Morais-Cabral, J. H., Kaufman, A. & MacKinnon, R. (2001). Chemistry of ion coordination and hydration revealed by a K^+ channel-Fab complex at 2.0 Å resolution. *Nature*, **414**, 43–48.
7. Alcayaga, C., Cecchi, X., Alvarez, O. & Latorre, R. (1989). Streaming potential measurements in Ca^{2+}-activated K^+ channels from skeletal and smooth muscle. Coupling of ion and water fluxes. *Biophys. J.* **55**, 367–371.
8. Morais-Cabral, J. H., Zhou, Y. F. & MacKinnon, R. (2001). Energetic optimization of ion conduction rate by the K^+ selectivity filter. *Nature*, **414**, 37–42.
9. LeMasurier, M., Heginbotham, L. & Miller, C. (2001). KcsA: it's a potassium channel. *J. Gen. Physiol.* **118**, 303–313.
10. Heginbotham, L. & MacKinnon, R. (1993). Conduction

properties of the cloned Shaker K^+ channel. *Biophys. J.* **65**, 2089–2096.
11. Eisenman, G., Latorre, R. & Miller, C. (1986). Multi-ion conduction and selectivity in the high-conductance CA^{++}-activated K^+ channel from skeletal muscle. *Biophys. J.* **50**, 1025–1034.
12. Hendrickson, W. A. (1991). Determination of macromolecular structures from anomalous diffraction of synchrotron radiation. *Science*, **254**, 51–58.
13. Phillips, J. C. & Hodgson, K. O. (1980). The use of anomalous scattering effects to phase diffraction patterns from macromolecules. *Acta Crystallog. sect. A*, **36**, 856–864.
14. Collaborative Computational Project number 4 (1994). The CCP4 suite: programs for protein crystallography. *Acta Crystallog. sect. D*, **50**, 760–763.
15. Tessman, J. R. & Kahn, A. H. (1953). Electronic polarizabilities of ions in crystals. *Phys. Rev.* **92**, 890–895.
16. Hess, P. & Tsien, R. W. (1984). Mechanism of ion permeation through calcium channels. *Nature*, **309**, 453–456.
17. Almers, W. & McCleskey, E. W. (1984). Non-selective conductance in calcium channels of frog muscle: calcium selectivity in a single-file pore. *J. Physiol.* **353**, 585–608.
18. Hille, B. & Schwarz, W. (1979). K channels in excitable cells as multi-ion pores. *Brain Res. Bull.* **4**, 159–162.
19. Jencks, W. P. (1987). *Catalysis in Chemistry and Enzymology*, Dover, New York, NY.
20. Doyle, D. A., Cabral, J. M., Pfuetzner, R. A., Kuo, A. L., Gulbis, J. M., Cohen, S. L. *et al.* (1998). The structure of the potassium channel: molecular basis of K^+ conduction and selectivity. *Science*, **280**, 69–77.
21. Otwinowski, Z. & Minor, W. (1997). Processing of X-ray diffraction data collected in oscillation mode. *Methods Enzymol.* **276**, 307–326.
22. Jones, T. A., Zou, J. Y., Cowan, S. W. & Kjeldgaard, M. (1991). Improved methods for building protein models in electron-density maps and the location of errors in these models. *Acta Crystallog. sect. A*, **47**, 110–119.
23. Brunger, A. T., Adams, P. D., Clore, G. M., DeLano, W. L., Gros, P., Grosse-Kunstleve, R. W. *et al.* (1998). Crystallography and NMR system: a new software suite for macromolecular structure determination. *Acta Crystallog. sect. D*, **54**, 905–921.
24. Kleywegt, G. J. & Jones, T. A. (1996). xdlMAPMAN and xdlDATAMAN—programs for reformatting, analysis and manipulation of biomacromolecular electron-density maps and reflection data sets. *Acta Crystallog. sect. D*, **52**, 826–828.
25. Kraulis, P. J. (1991). MOLSCRIPT: a program to produce both detailed and schematic plots of protein structures. *J. Appl. Crystallog.* **24**, 946–950.
26. Esnouf, R. M. (1999). Further additions to MolScript version 1.4, including reading and contouring of electron-density maps. *Acta Crystallog. sect. D*, **55**, 938–940.
27. Merritt, E. A. & Bacon, D. J. (1997). Raster3D: photorealistic molecular graphics. *Methods Enzymol.* **277**, 505–524.

Edited by D. Rees

(Received 27 June 2003; received in revised form 4 September 2003; accepted 5 September 2003)